



Autonomous damage recognition in visual inspection of laminated composite structures using deep learning



Sakineh Fotouhi^a, Farzad Pashmforoush^b, Mahdi Bodaghi^c, Mohamad Fotouhi^{a,*}

^a School of Engineering, University of Glasgow, Glasgow G12 8QQ, UK

^b Department of Mechanical Engineering, University of Maragheh, Maragheh, Iran

^c Department of Engineering, School of Science and Technology, Nottingham Trent University, Nottingham NG11 8NS, UK

ARTICLE INFO

Keywords:

Composite materials
Damage detection
Deep learning
Visual inspection

ABSTRACT

This study proposes the exploitation of deep learning for quantitative assessment of visual detectability of different types of in-service damage in laminated composite structures such as aircraft and wind turbine blades. A comprehensive image-based data set is collected from the literature containing common microscale damage mechanisms (matrix cracking and fibre breakage) and macroscale damage mechanisms (impact and erosion). Then, automated classification of the damage type and severity was done by pre-trained version of AlexNet that is a stable convolutional neural network for image processing. Pre-trained ResNet-50 and 5 other user-defined convolutional neural networks were also used to evaluate the performance of AlexNet. The results demonstrated that employing AlexNet network, using the relatively small image dataset, provided the highest accuracy level (87%–96%) for identifying the damage severity and types in a reasonable computational time. The generated knowledge and the collected image data in this paper will facilitate further research and development in the field of autonomous visual inspection of composite structures with the potential to significantly reduce the costs, health & safety risks and downtime associated with integrity assessment.

1. Introduction

Composite materials have the advantages of high strength to weight ratio, good vibration damping ability, and high wear, creep, corrosion, fatigue and temperature resistances [1]. Due to these excellent properties, composite materials are widely used in different sectors such as civil, aerospace, wind energy, oil & gas, automotive, etc. Despite the advantages, an important problem for composites is their susceptibility to damage that can result in fatigue life reduction or catastrophic failure if unseen [2–4]. Most polymeric composite materials have brittle and laminated nature, making them susceptible and sensitive to damage. As a result, in safety critical applications, engineers are forced to apply conservative design approaches based on low allowable strains. For example, maximum allowable design strains can be as low as 0.1% for carbon fibre composites, despite maximum fibre failure strains of up to 2% [5,6]. Different damage mechanisms can happen in composite components, ranging from microscopic matrix cracking and fibre breakage to large, and critical impact damage [7,8]. These damage mechanisms can be induced by operational loadings during service or unwanted events during manufacturing

and assembly. Fig. 1 shows examples of in-service surface damage in composite structures. Among these surface damage mechanisms, impact damage is very common for the aerospace industry, whereas erosion of the leading edge is observed frequently in composite wind turbine blades. These in-service damage mechanisms are likely to contain different microscale damage mechanisms such as fibre breakage, matrix cracking, and delamination [9,10]. Fig. 2 shows a schematic of these microscale damage mechanisms for a laminated composite under low velocity impact.

If a composite material component is damaged, the size, shape, depth, type, and extent of the damage and its restitution approach should be determined. A typical repair procedure and an example of barely visible impact damage repair in a laminated composite is shown in Fig. 3.

Of immediate importance for the composite integrity and serviceability evaluation is the ability to identify the damage and measure its extent by an appropriate non-destructive inspection (NDI) technique. Several NDI techniques are used in the composite field, including visual testing or visual inspection [12], optical testing [13], ultrasonic testing [14], acoustic emission testing [15], thermographic

* Corresponding author.

E-mail address: Mohammad.fotouhi@glasgow.ac.uk (M. Fotouhi).

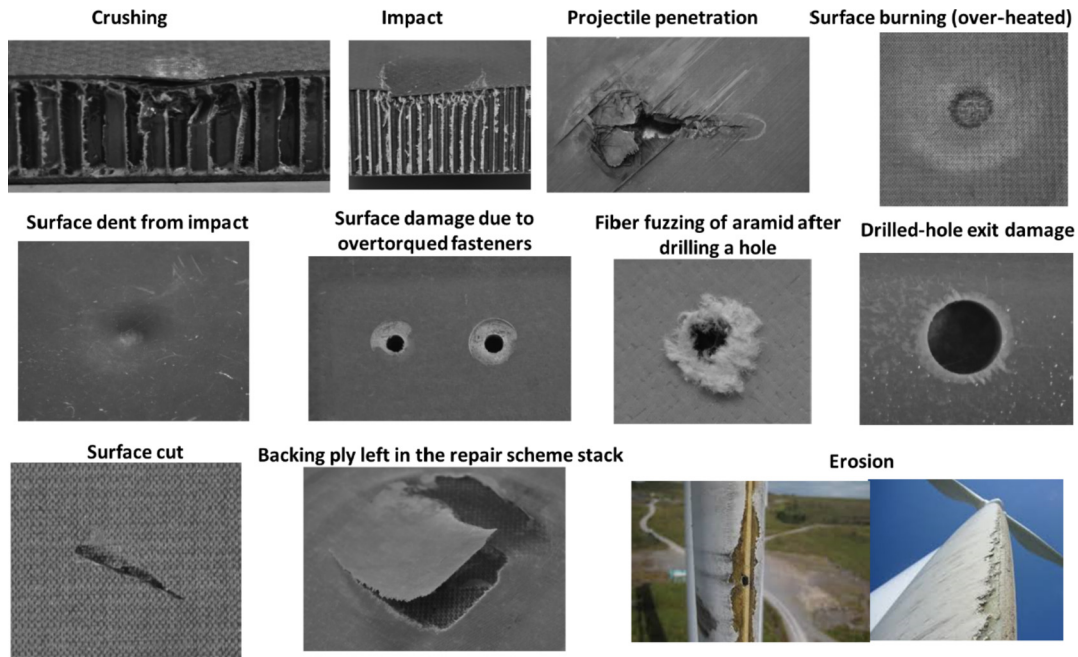


Fig. 1. In-service surface damage examples in laminated composite structures [11].

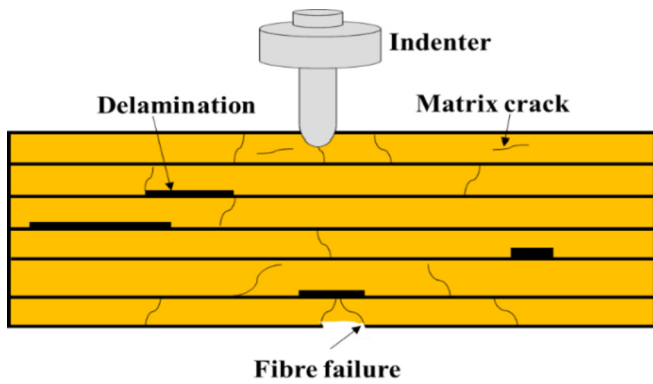


Fig. 2. Main microscale damage mechanisms in laminated composites under impact loadings.

testing [16], infrared thermography testing [17], radiographic testing [18], acousto-ultrasonic [19], shearography testing [20], electromagnetic testing [21], etc. Most, if not all, of these NDI techniques require high levels of operator experience to successfully apply and interpret the results. These NDI techniques are usually expensive, time-consuming, and sophisticated, and the component has to be out of service for the inspection; thus causing further inconvenience. These precautions reduce the inherent performance advantages of composites and even make them unsuitable for many applications in which

catastrophic failure cannot be tolerated. As a result, there is a need for cost-effective and reliable inspection solutions to ensure safety, reliability, and longer service life of composite structures.

Visual inspection is the main method of routine inspection for different composite structures in aircraft, wind turbine blades, and many other sectors [12]. It is considered the quickest, cheapest, and most common method to find cracks or surface dents, and it can reduce the need for a full scan by other expensive and complicated NDI techniques, or in some cases, it can reduce the need for other types of NDI if no critical damage is revealed. If a visual inspection reveals critical damage to a composite structure, inspectors may request non-destructive testing such as Ultrasonic to determine the extent of the associated subsurface damage to determine the need for repair or replacement. For instance, over 80 percent of inspections on large aircraft are visual inspections, rope access visual inspection of composite wind turbine blades is also the most common inspection practice [22].

Therefore, visual inspection is the most used and least expensive and quickest method for assessing the condition of safety-related failures on critical composite structures. Consequently, reliable, and accurate visual inspection is vital to the continued safe operation of composite structures. Currently, visual inspection is mainly done by skilled operators, so the accuracy depends on the operator and there are health and safety risks. There are plenty of factors such as lighting, inspection time, inspector tiredness and experience, and environmental conditions which influence the reliability of visual inspection and probability of detection [23,24].

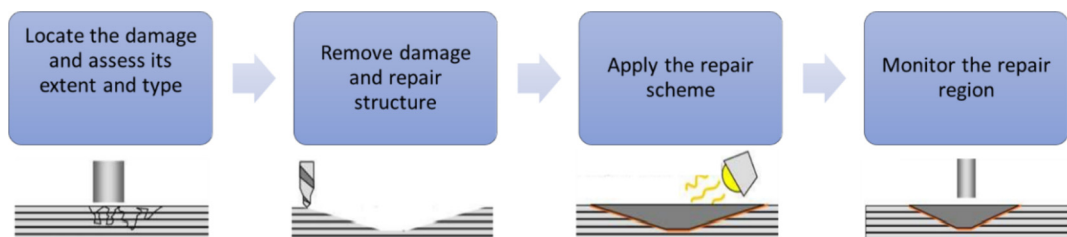


Fig. 3. A typical composite structure repair procedure, and an example of barely visible impact damage repair process.

Advances in automation [25], data analytics [26,27], image acquisition techniques [28,29], artificial intelligence technologies [30,31], and computationally efficient smartphones, inexpensive high-resolution cameras and drones [32], have recently enabled the capacity to build automated visual inspection systems that can surpass human accuracy. A schematic of recent advances that enables the potential of next-generation autonomous visual inspection systems in composite structures is shown in Fig. 4.

High-quality algorithms and high-quality data for training those algorithms are essential factors that need to be established to develop autonomous visual inspection systems in composite structures. In this paper, the efficiency of artificial neural network (ANN) algorithms is evaluated for identifying the damage types and severities in visual inspection of composite structures. ANNs are a subclass of semi-supervised machine learning techniques, and they have been successfully used in several studies for damage classification of composite materials. Among various ANNs, convolutional neural networks (CNNs) have attracted high attention in effectively handling image-based data due to their ability in extracting deep patterns. The ANNs also take the advantages of dataset augmentation and transfer learning that make it possible to train accurate models when limited data is available. Several CNN architectures have been proposed for image classification including AlexNet [33], FuseNet [34], ZF Net [35], and ResNet [36]. Saeed et al. [37] applied AlexNet CNN for thermography defect detection and depth estimation of 3D printed Carbon Fibre Reinforced Plastics (CFRPs), based on the pulsed thermography images taken from the samples with embedded air pockets. The proposed method identified embedded defects without any human interventions with high accuracy above 88%. Bang et al. [38] also employed CNN and transfer learning for the classification of thermographic images of carbon/epoxy composite specimens. They used Inception V2 architecture to identify the presence of the defects as well as their shapes (i.e. spheroidal, circular and irregularly shaped defects). Gong et al. [39] applied CNN for inclusion defect detection of aeronautics composite materials based on the X-ray images. According to the obtained results, the proposed CNN could accurately extract X-ray images features and detect the presence of the inclusion. There are some other studies towards the application of CNN in damage

detection of composite materials which are based on non-image data generated from various inspection techniques, such as ultrasonic signals [40], structural vibration responses [41], lamb waves [42], distributed strains [43] and PZT sensors [44]. For example, Meng et al. [40] successfully used CNN for the classification of ultrasonic signals from CFRP samples to classify the voids and delamination defects.

In previous applications of CNNs on image-based data, the images were obtained through NDT techniques such as thermography and X-ray [37–39] from defects that occur during the manufacturing of composite materials. These studies were only focused on single class detection models (i.e., the presence of defects or not), without consideration of damage types and severity. A thorough search of the relevant literature yielded that machine learning-based image processing has not been exploited in identification and classification of visually inspected in-service damage mechanisms in composite structures. Despite many research publications on in-service induced damage in composite structures, there is no comprehensive publication summarising different visible damage mechanisms on composite structures.

To address the aforementioned challenges, this paper introduces a novel exploitation of CNNs for quantitative assessment of image-based data taken from visual observation of different types of in-service damage in laminated composite structures. A comprehensive image-based data set of common in-service damage mechanisms (matrix cracking, fibre breakage, impact, and erosion) were collected from the literature. The data set was successfully used to train the CNNs to evaluate their accuracy and robustness in identifying the various in-service damage mechanisms and their severity (for example high energy or low energy impacts). Given the CNNs ability to detect different damage mechanisms on diverse material combinations, the introduced system can be implemented for a wide range of industries such as aerospace, wind, civil and oil & gas.

2. Methodology

2.1. Convolutional neural network

Deep learning is a subset of machine learning that mimics the behaviour of the human brain in processing data by learning tasks directly from sound, text, and images. CNN is a type of deep learning, developed to automatically and adaptively process structured arrays of data [37,45]. CNN consists of an input layer, several hidden layers, and an output layer. The hidden layers themselves include convolutional layers, pooling layers, activation layers, fully connected layer, and Soft-max classification layer. The convolution layers consist of a set of filters (with learnable weights), which are exerted on the input image to extract its main features. An example of convolution operation with a 3 × 3 filter, stride size of two and padding size of one is illustrated in Fig. 5. As depicted, the convolution operation convolves the input layer

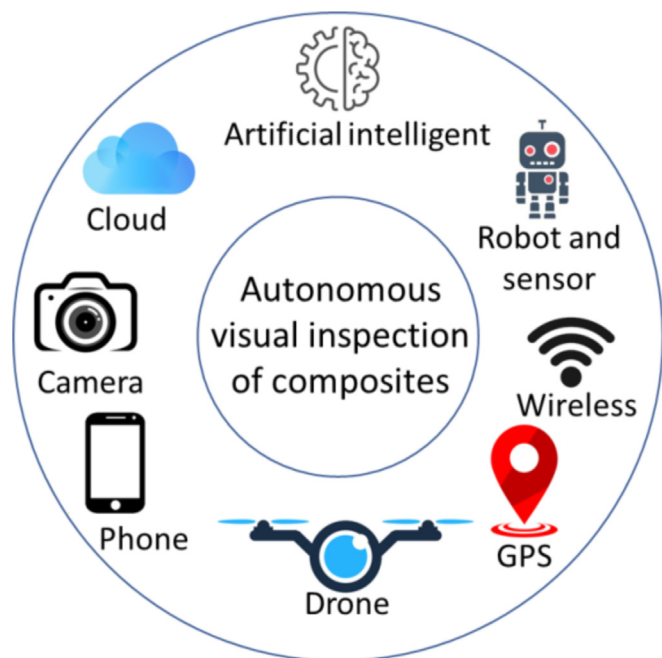


Fig. 4. A schematic of recent advances that enables the potential of next-generation autonomous visual inspection systems.

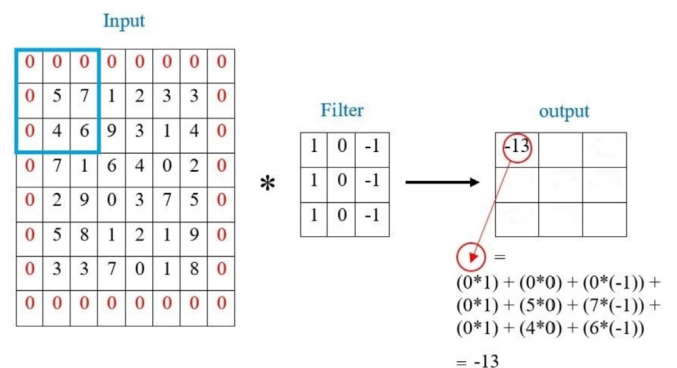


Fig. 5. An example of convolution and padding operations with a 3 × 3 filter, stride size of two and padding size of one.

ers by sliding the filter through the input data horizontally and vertically, calculates the dot product of the weights and the input, and then adds a bias term. The step size of the filter movement is determined by the stride size. As shown in Fig. 5, the convolution operation is accompanied by a padding operation, which inserts additional layers to the image border. This operation leads to more accurate image analysis since it prevents data shrinkage and information loss in the image borders. Without padding, the input data progressively shrinks every time after the convolution operation. Also, the pixels in the image borders get covered (by the filters) only one time, while the filters continuously cover the middle pixels. This leads to the loss of information in the image borders. To overcome these problems, the application of padding operation is of great importance for accurate image classification. After convolution and padding operations, the activation layer adds some non-linearity to the network, since most of the real-world problems are non-linear [39]. For example, rectified linear unit (ReLU) activation function applies a threshold operation to each element, where any input value less than zero is set to zero. The pooling layer is then applied to progressively decrease the size of the layers (by performing the down-sampling operation), which leads to the reduction in the number of iterations, weights and consequently the computation cost. An example of pooling operation with a 2×2 filter and stride size of two is demonstrated in Fig. 6. Through these steps, the input image is converted to a high-level feature map which is further processed by the fully connected layer that connects every neuron in one layer to every neuron in another layer, as shown in Fig. 7. Finally, the Softmax layer is employed to classify the input images. In a typical CNN, high precision image classification requires a very large labelled dataset, with a massive amount of training data with different possible variations in size, orientation, number of objects, etc [46]. Hence, application of pre-trained models (transfer learning) is of great importance for efficient classification purposes. In transfer learning, the network has already been trained by a large dataset that includes various classes of objects (not essentially relevant to the specific target task). By fine tuning this pre-trained network, it can be employed as a starting point to learn a new task, in accordance with the classification goal. Fig. 8 shows flowchart of the damage classification process applied in this paper.

2.2. AlexNet

The superiority of AlexNet CNN architecture over others in exploitation of transfer learning for the classification of defects in CFRP thermograms [37] and satellite image data [47] has been demonstrated. AlexNet network is one of the most widely used CNN architectures that has been successfully trained on more than a million images [33]. AlexNet network can learn rich feature representations for various types of images, which eliminates the need for time-consuming training of the network from the scratch. Furthermore, stable implementation of pre-trained version of AlexNet is developed in Matlab [48] that is used in this study. AlexNet architecture is illus-

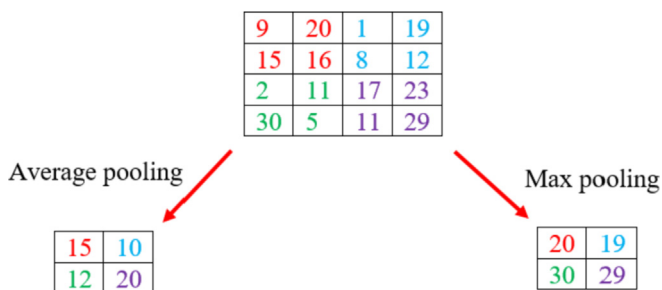


Fig. 6. An example of pooling operation with a 2×2 filter and stride size of two.

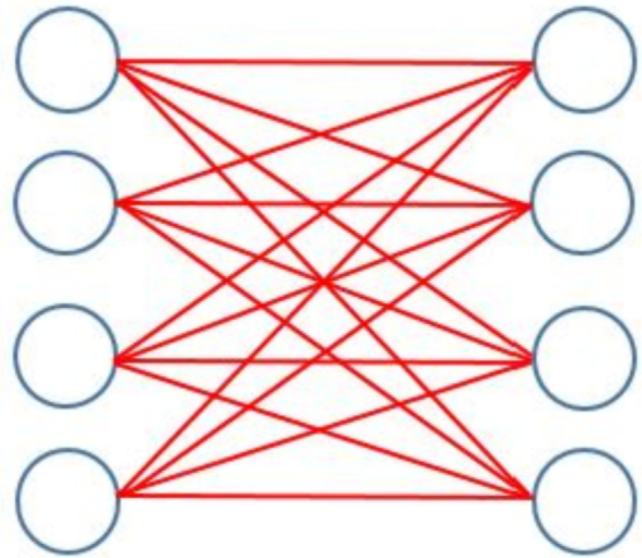


Fig. 7. Schematic representation of fully connected layers.

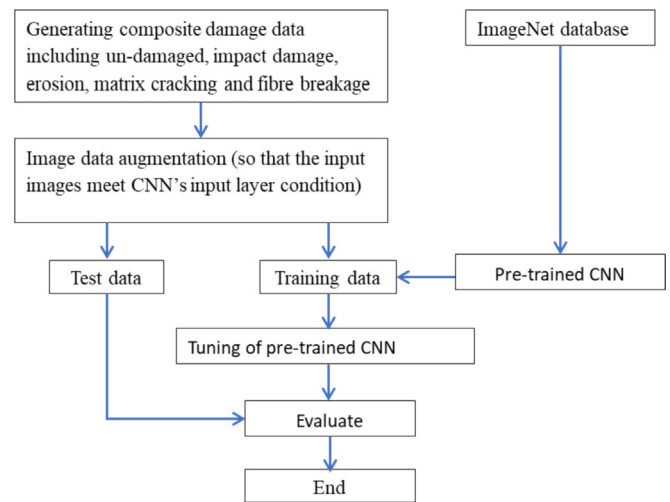


Fig. 8. Flowchart of the damage classification process.

trated in Fig. 9, which contains five convolutional layers, three pooling layers, three fully connected layers and one Softmax layer.

3. Results and discussion

3.1. Damage mechanisms data set

Fig. 10 summarises the collected image data for this study including un-damaged, impact damage, erosion, matrix cracking and fibre breakage. A comprehensive set of images were collected from the literature from laminated composite materials with different thicknesses, materials, layups, texture, etc. The low and high impact damage types were distinguished from each other visually, where the images with a significant visible fibre breakage were categorised as high energy. A dataset containing 20, 24, 16, 52, 25, 39, 28 and 24 images was collected for matrix cracking (Fig. 11), fibre breakage (Fig. 12), un-damaged (Fig. 13), low energy impacted face (Fig. 14), high energy impacted face (Fig. 15), low energy back face (Fig. 16), high energy back face (Fig. 17), and erosion (Fig. 18), respectively. The impact and erosion related images were collected from the literature

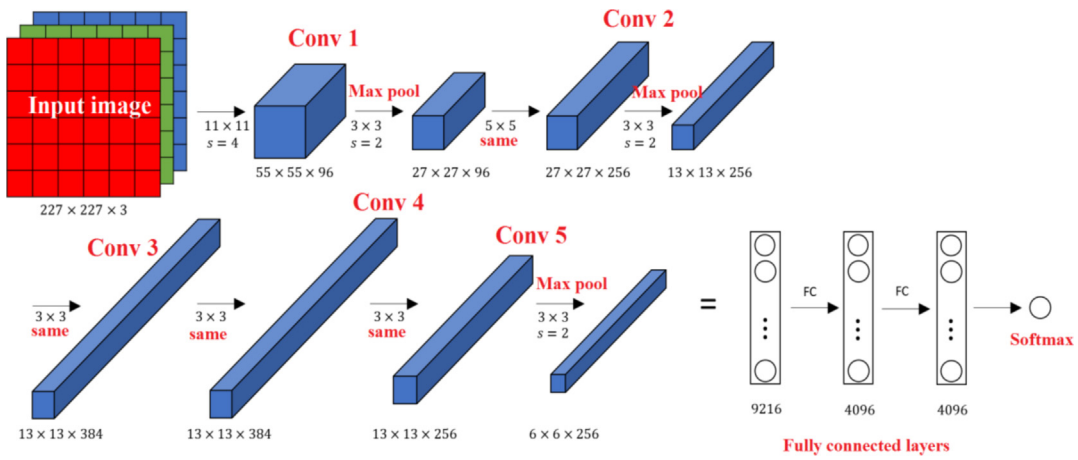


Fig. 9. Architecture of AlexNet network.

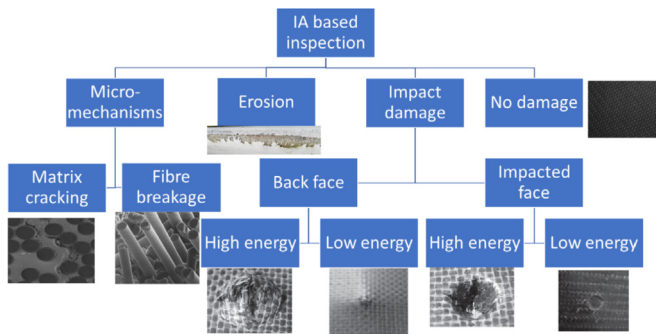


Fig. 10. Summary of the collected data, including no damage, impact damage (back and impacted faces, with low and high energy levels), erosion, matrix cracking and fibre breakage.

[41–63], and [64–69], respectively. The matrix cracking and fibre breakage pictures are taken from the literature [70–76].

3.2. Classification of microscale damage mechanisms

The performance of AlexNet network is assessed in the classification of microscale damage mechanisms such as matrix cracking and

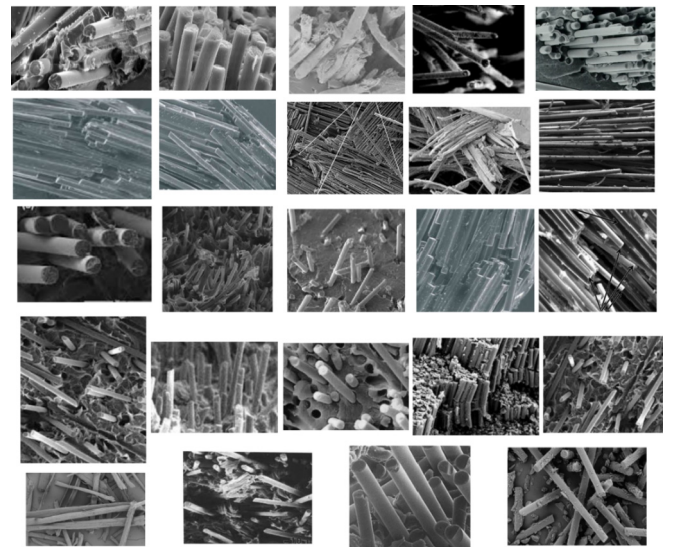


Fig. 12. Microscopic damage dataset for fibre breakage.

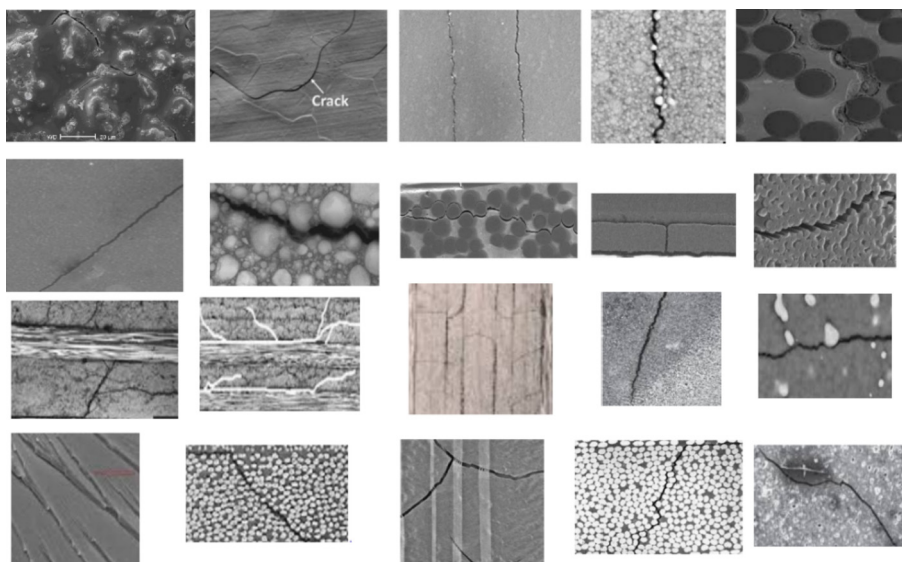


Fig. 11. Microscopic damage dataset for matrix cracking.



Fig. 13. Un-damaged composites dataset.

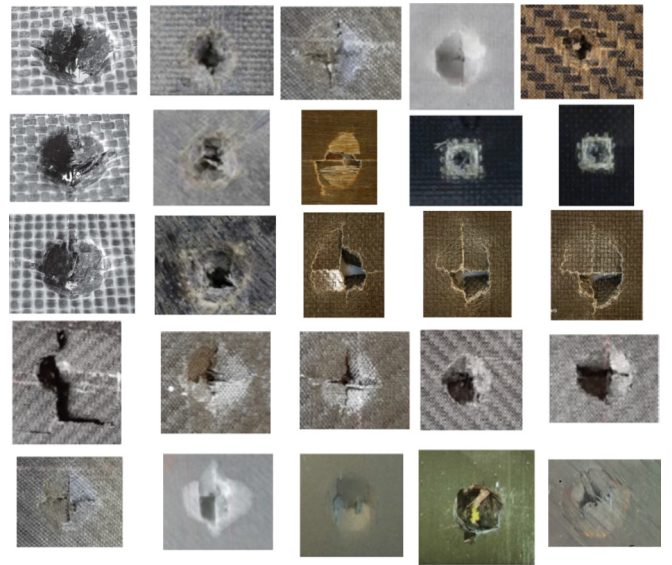


Fig. 15. High energy impacted face impact damage dataset.

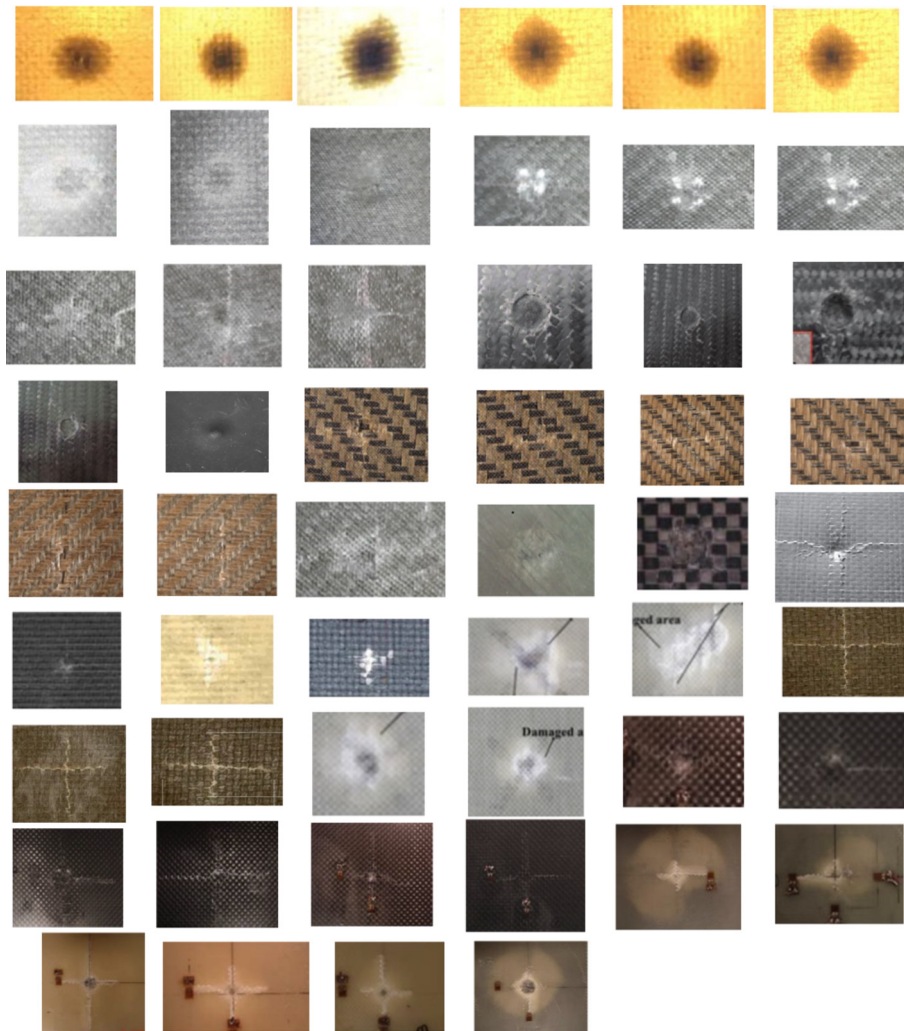


Fig. 14. Low energy impacted face impact damage dataset.

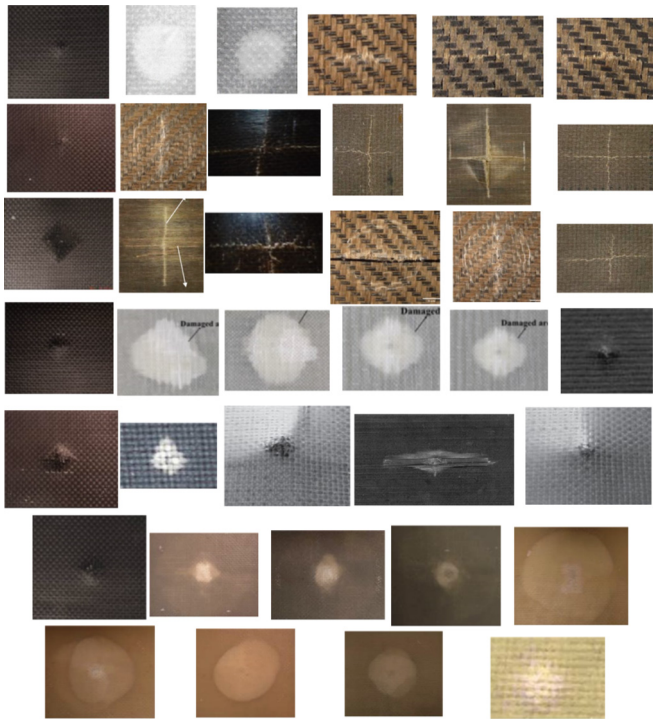


Fig. 16. Low energy back face impact damage dataset.

fibre breakage. 75% of the dataset images were randomly selected for training purposes, and 25% were selected for validation purposes. First of all, the images were resized to meet the Alexnet input layer condition (i.e. image sizes of $227 \times 227 \times 3$) using an augmented image datastore algorithm. Then, these images were used for training the deep learning network, using an initial learning rate of 0.0002. After training the network, its performance was evaluated by classification of the validation images. In this case, the best validation accuracy was 91%, obtained in the case of a learning rate of $5e-5$, as shown

in Fig. 19. Some samples of the validation images classified by the network are depicted in Fig. 20. Finally, the network was implemented for the classification of unseen images. As illustrated in Fig. 21, the network has successfully classified the unseen images with a high accuracy level, where all the six unseen images have been accurately classified.

In order to evaluate the performance of AlexNet network, it is compared with five other user-defined neural networks and Resnet-50 [77] that is an established image processing CNN and was pre-trained with the ImageNet database [78]. The architecture of the user-defined networks (i.e. the number of convolutional layers, number of pooling layers, number and size of filters, etc.) was determined based on the data available in the literature [37–39,41], as summarised in Table 1. The obtained results (i.e. the validation accuracy and CPU evaluation time) from classification of microscale damage mechanisms are listed in Table 2. It should be mentioned that all the computations were performed by MATLAB on Intel Core i7 CPU @ 1.6 GHz and RAM 4 GB. As illustrated in Table 2, among the user-defined networks, the highest accuracy is 84.62%, belonging to Net_4, with a CPU time of 508.92 s; while the least accuracy is 61.54%, belonging to Net_1, with a CPU time of 45.3 s. The accuracy of Resnet-50 CNN is 83.33%, with a CPU time of 153.63 s. Comparing these results with those of AlexNet network (i.e. accuracy of 91.67% and CPU time of 71.91 s) reveals the high performance of AlexNet network in the classification of damage mechanisms, in terms of accuracy and computational time efficiency. As a sample, the validation and classification results for networks Resnet-50, Net_1 and Net_4 are illustrated in Figs. 22–24, respectively.

3.3. Classification of macroscopic damage mechanisms

In this section, the performance of AlexNet network is illustrated in the classification of impact damage, erosion, and un-damaged samples. The severity of the impact damage (i.e. high energy and low energy impact damage) was also distinguished by the network. Some sample classification results of the damage severity for the impacted face are depicted in Fig. 25, and the obtained accuracy is shown in Fig. 26. As shown, the validation accuracy is 96%, achieved in the case of

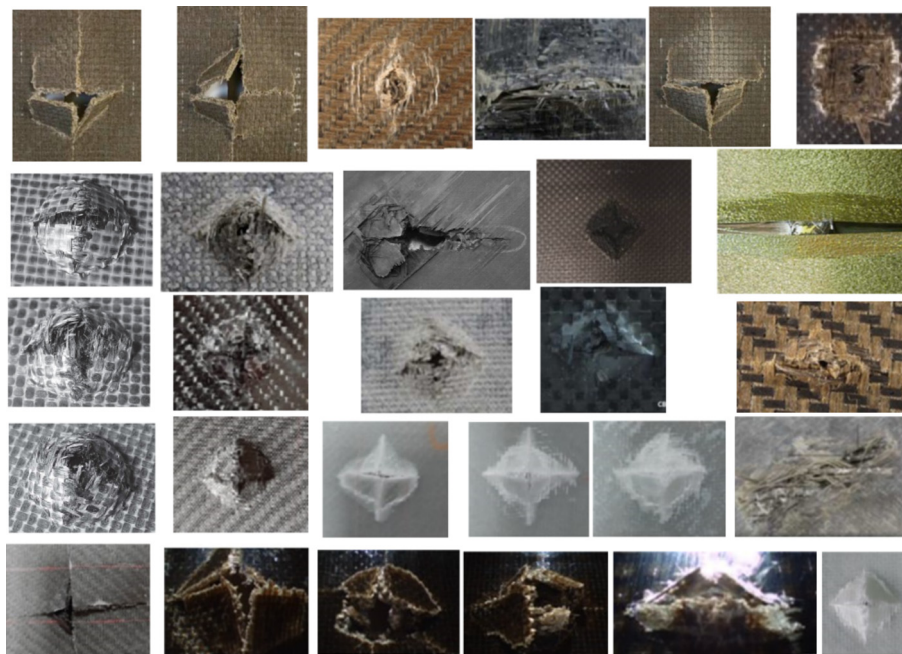


Fig. 17. High energy back face impact damage dataset.

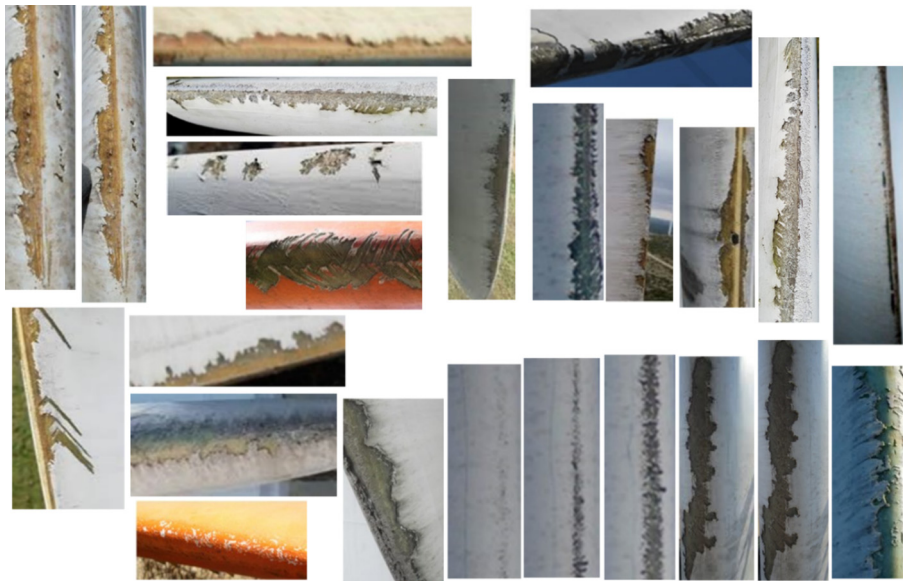


Fig. 18. Erosion damage dataset for wind turbine blades.

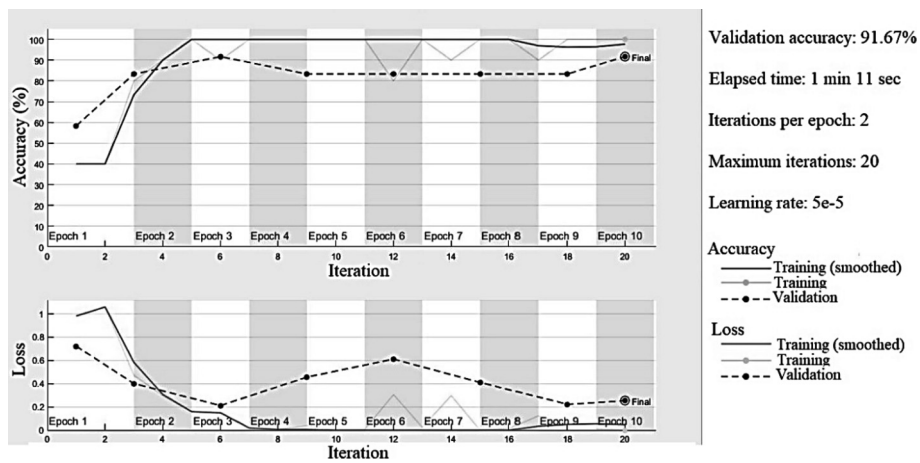


Fig. 19. The accuracy of AlexNet network in the classification of validation images.

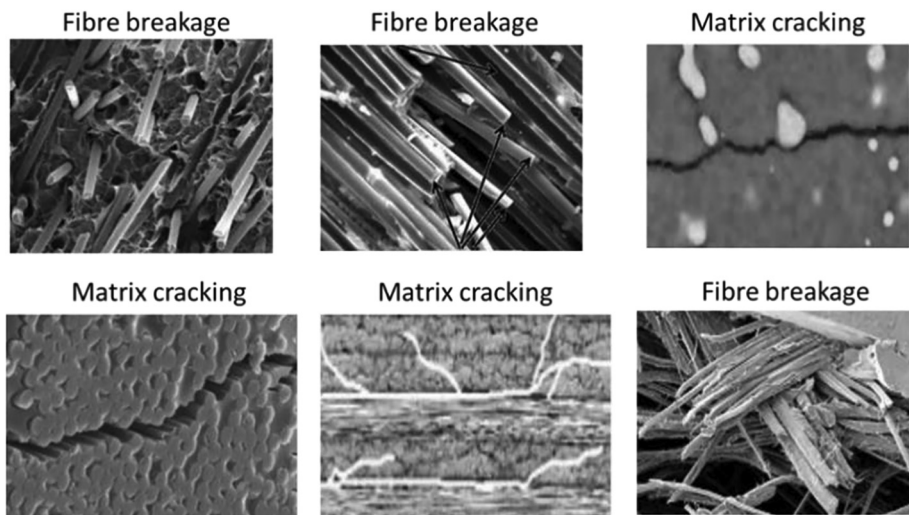


Fig. 20. Samples of the validation images classified by AlexNet network.

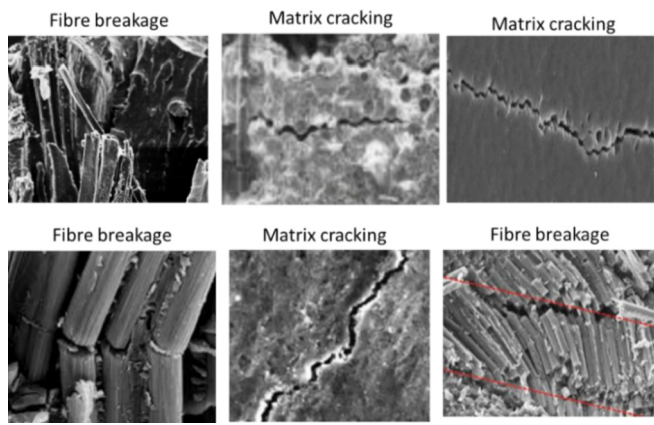


Fig. 21. Classification of unseen images of microscopic damage mechanisms.

Table 1

Architecture of user-defined neural networks.

No.	Convolutional layers	Pooling layers
Net_1	one convolutional Layer: L1: 64 filters with size of 5×5 , stride: 2; padding: 1	one pooling layer: pool size: 2×2 ; stride: [1 1]; padding: [0 0 0 0];
Net_2	three convolutional Layers: CL1: 16 filters with size of 5×5 , stride: 2; padding: 0 CL2: 64 filters with size of 3×3 ; stride: 2, padding: 1 CL3: 128 filters with size of 3×3 ; stride: 1; padding: 1	one pooling layer: pool size: 2×2 ; stride: [2 2]; padding: [0 0 0 0];
Net_3	three convolutional Layers: CL1: 64 filters with size of 5×5 , stride: 2; padding: 1 CL2: 128 filters with size of 5×5 ; stride: 2, padding: 2 CL3: 256 filters with size of 3×3 ; stride: 1; padding: 1	three pooling layers: pool size: 3×3 ; stride: [2 2]; padding: [0 0 0 0];
Net_4	five convolutional Layers: CL1: 64 filters with size of 10×10 , stride: 1; padding: 0 CL2: 128 filters with size of 5×5 ; stride: 2, padding: 1 CL3: 256 filters with size of 5×5 ; stride: 2; padding: 1 CL4: 256 filters with size of 3×3 ; stride: 2; padding: 2 CL5: 64 filters with size of 3×3 ; stride: 1; padding: 1	three pooling layers: pool size: 2×2 ; stride: [2 2]; padding: [0 0 0 0];
Net_5	five convolutional Layers: CL1: 64 filters with size of 10×10 , stride: 1; padding: 0 CL2: 128 filters with size of 5×5 ; stride: 2, padding: 1 CL3: 128 filters with size of 3×3 ; stride: 2; padding: 1 CL4: 256 filters with size of 3×3 ; stride: 2; padding: 2 CL5: 64 filters with size of 1×1 ; stride: 1; padding: 1	five pooling layers: pool size: 3×3 ; stride: [2 2]; padding

Table 2

Accuracy and CPU time of user-defined neural networks and AlexNet network.

Network type	Accuracy	CPU evaluation time (second)
AlexNet	91.67%	71.91
Resnet-50	83.33%	153.63
Net_1	61.54%	45.30
Net_2	69.23%	56.59
Net_3	76.92%	70.82
Net_4	84.62%	508.92
Net_5	76.92%	543.14

the learning rate of 0.0001. It should be mentioned that the item marked by a red circle is wrongly classified by the network. This object belongs to low impact energy category, but it is classified as high impact energy, which is due to its similar features to high energy damage.

Followed by the training and validation processes, AlexNet network was implemented for the classification of some unseen images, as illustrated in Fig. 27. The obtained results indicate the promising performance of the network for accurate classification of the damage severity for the impacted face. In the following, the network was used for the classification of the back face images. As illustrated in Figs. 28–30, yet again, the network could successfully classify the damage severity for the back face impact, with an accuracy level of 87%.

AlexNet network was also used to distinguish the various macroscopic damage mechanisms, i.e. impact, erosion, and un-damaged. As illustrated in Fig. 31, the best validation accuracy is 93%, achieved in the case of a learning rate of 0.0001. Some sample classification results of validation images and unseen images are depicted in Figs. 32 and 33. Again, the network demonstrated a promising performance and could accurately classify the various macroscopic damage mechanisms, as well as the un-damaged case.

Finally, AlexNet network was used to discriminate the impacted face and back face images. The obtained validation accuracies for low and high energy impact cases of the impacted and back faces are respectively 78% and 73%, as depicted in Figs. 34 and 35. In this example, the classification accuracies are much less than those of the previous examples, which is due to the similar features between the impacted face images and the back face images. In other words, there are not many obvious discrepancies between the images, so that the features extracted by the network are not distinct enough, even by a naked eye, to yield accurate training and consequently reliable classification. This fact is better illustrated in Figs. 36 and 37, which demonstrate the classification of the impacted face and back face images. As shown, some items (marked by a red circle) are wrongly classified by the network. In such cases, it is required to train the network with a much larger and comprehensive dataset containing enough variations in extractable features.

3.4. Future research

This paper illustrated the potential of deep learning techniques in autonomous damage detection of impact and erosion in composite structures. However, there is a diverse range of damage types in composite structures, and different parameters such as environmental conditions, illumination, cleanliness, geometry, inspection angle and colour / finish that may influence the damage detectability using image processing. Therefore, further experimental and modelling research is required to develop a comprehensive and high-quality dataset for different damage types in composite structures and their affecting parameters for a reliable machine learning based autonomous inspection. More research needs to be done on measuring the surface damage size, correlating the visible damage on the surface to the extent of potential invisible damage, and to predict residual life of the structures considering the damage content. The probability of surface damage detection, and its relationship with surface damage size for visual inspection needs to be established to be used in design calculations of structural strength and durability.

4. Conclusion

In this study convolutional neural network (CNN) in conjunction with transfer learning was used for the classification of composite materials damage types and damage severity. For this purpose, the pre-trained AlexNet network, as one of the most accurate transfer learning methods, was implemented. The network was used for the

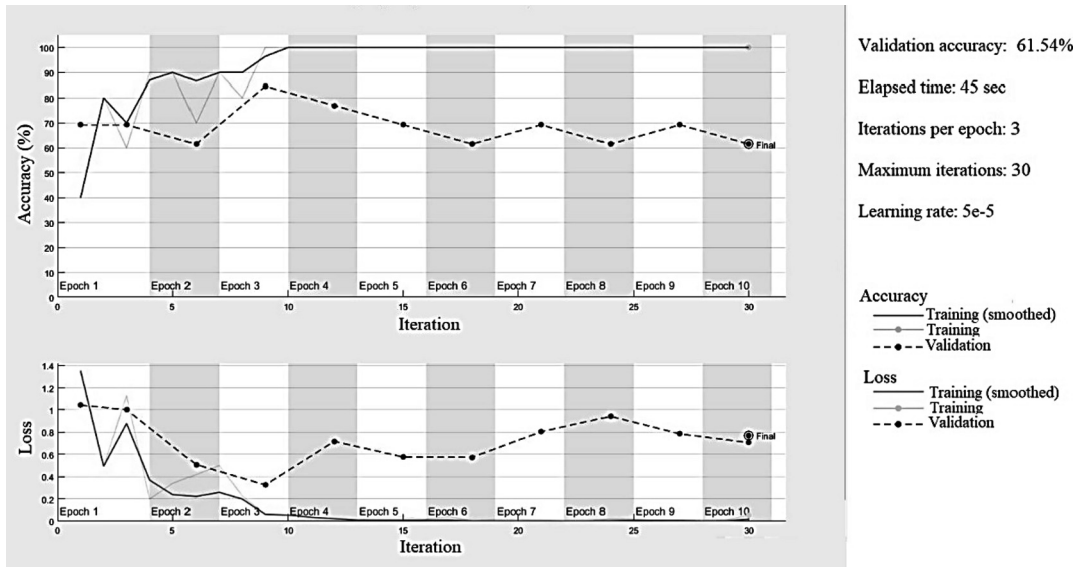


Fig. 22. The accuracy of Net_1 in the classification of validation images.

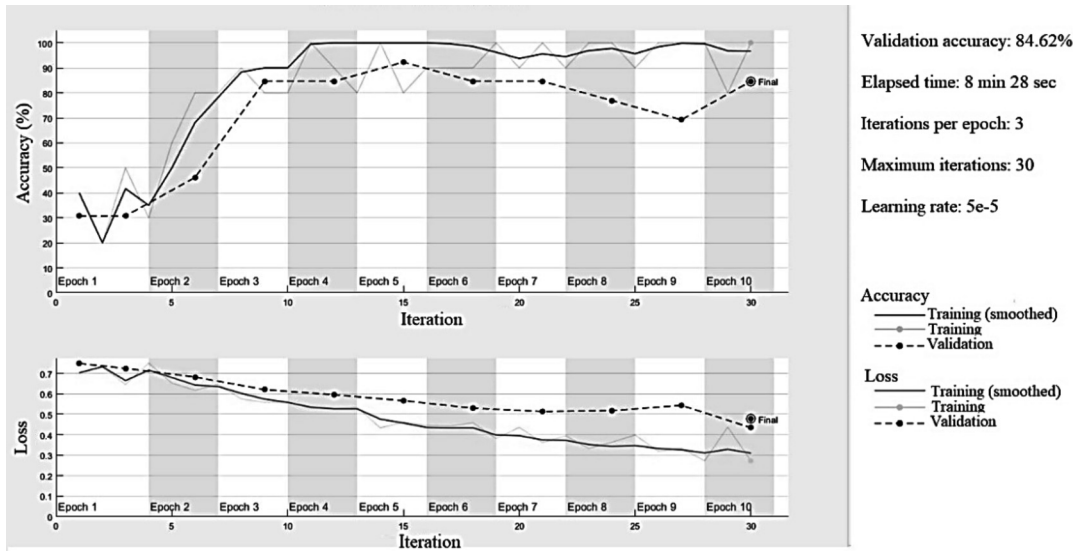


Fig. 23. The accuracy of Net_4 in the classification of validation images.

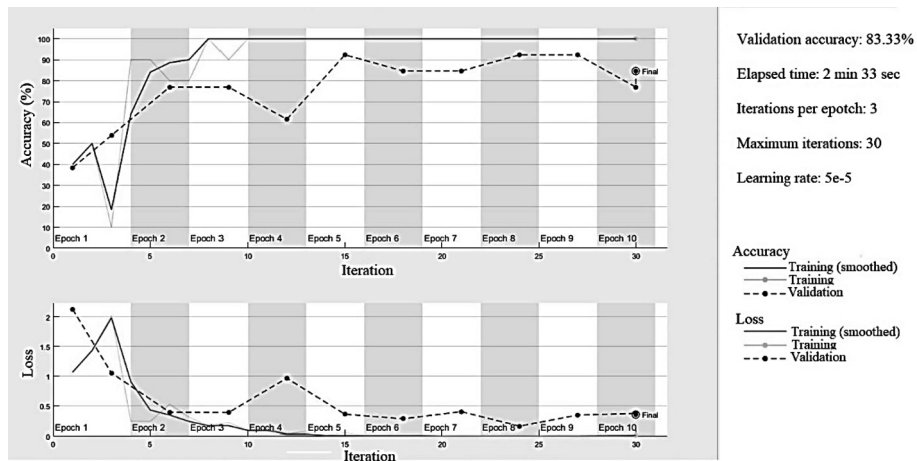


Fig. 24. The accuracy of Resnet-50 CNN in the classification of validation images.

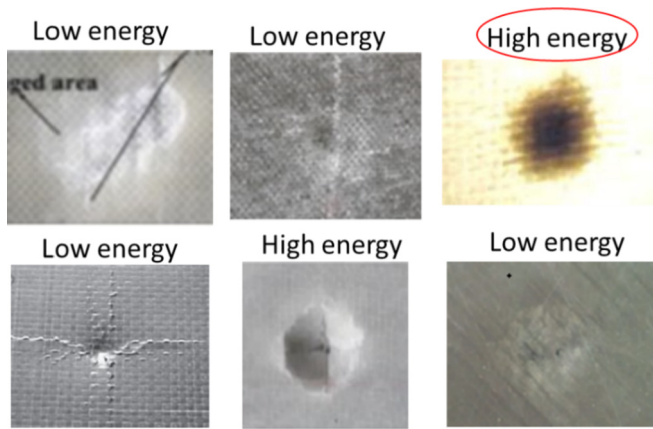


Fig. 25. Classification of damage severity (six sample validation images of the impacted face).

classification of a comprehensive set of image data collected from the literature for in-service damage mechanisms. In this regard, different conditions were investigated, including classification of microscopic damage mechanisms, matrix cracking and fibre breakage, macroscopic damage mechanisms (erosion and impact), as well as classification of damage severity. For evaluating AlexNet’s robustness, Resnet-50 CNN and 5 user-defined deep neural networks were also developed and utilised for identifying the microscale damage types. The following results and conclusions were drawn from the present study:

- AlexNet network outperformed Resnet-50 and the user-defined deep neural networks regarding the accuracy level for identifying the damage type in a reasonable computational time.
- The validation accuracy of the network strongly depends on the learning rate, where its optimum value was achieved using the trial and error method.
- The obtained accuracy in the classification of microscopic damage mechanisms (i.e. matrix cracking and fibre breakage) was 91%, achieved in the case of a learning rate of $5e-5$.
- For damage severity classification (i.e. low energy or high energy impact), the validation accuracy was 96% for the impacted side, and 86% for the back face. For the case of macroscopic damage type identification (i.e. erosion, impact and un-damaged), the best validation accuracy was 93%, achieved in the case of a learning rate of 0.0001.

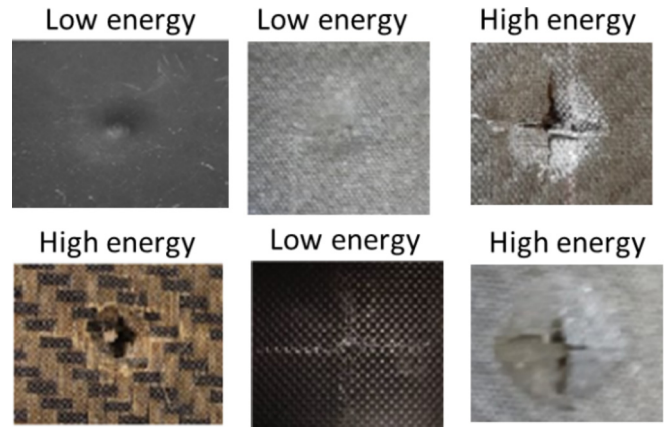


Fig. 27. Classification of damage severity for unseen images of the impacted face.

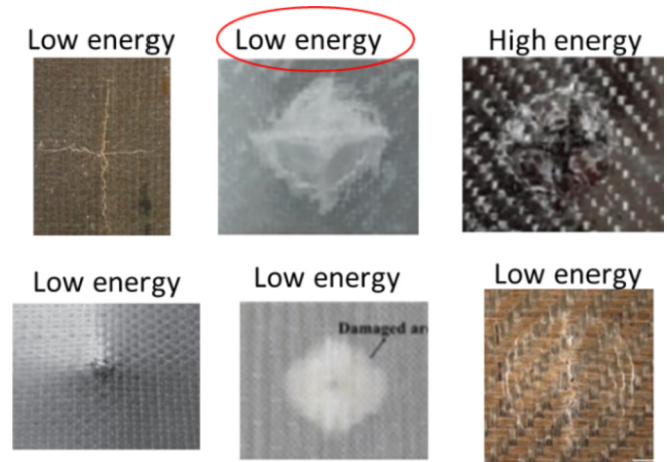


Fig. 28. Classification of damage severity (six sample validation images of the back face).

- In spite of AlexNet network’s high accuracy in the classification of various damage types and damage severity, it couldn’t accurately classify the damage side (i.e. impacted face or back face). The obtained accuracies for low and high energy impact cases were 78% and 73%, respectively. This can be related to the similar fea-

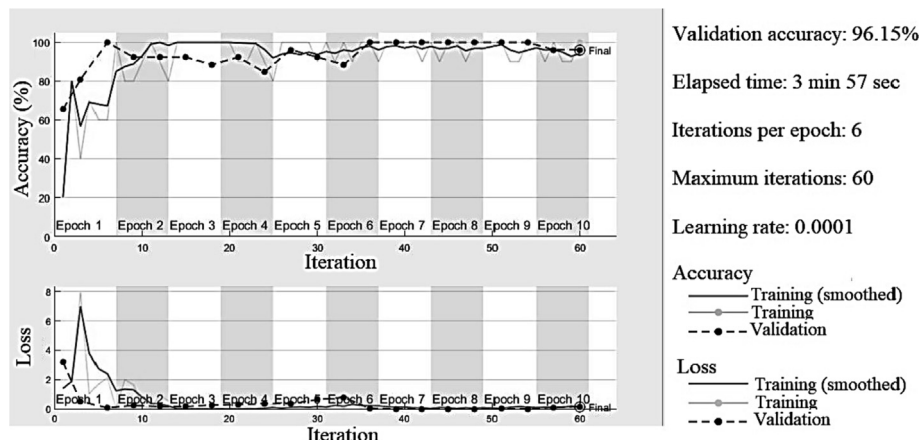


Fig. 26. Obtained validation accuracy for the classification of damage severity (the impacted face).

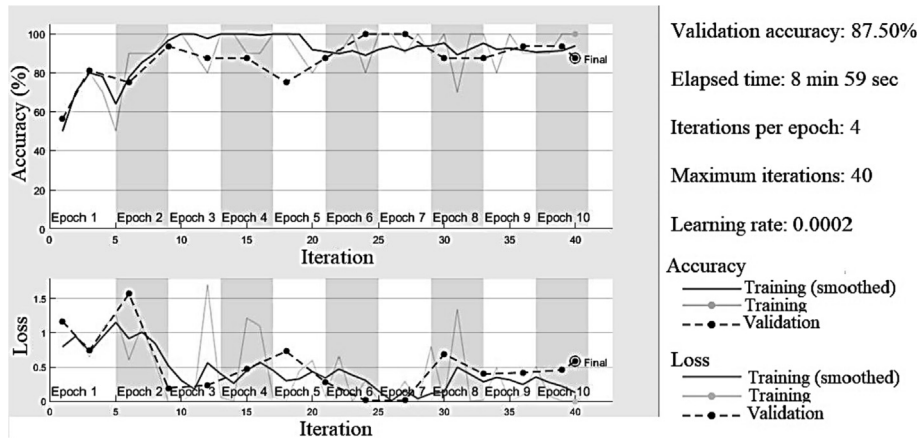


Fig. 29. Obtained validation accuracy for the classification of damage severity of the back face.

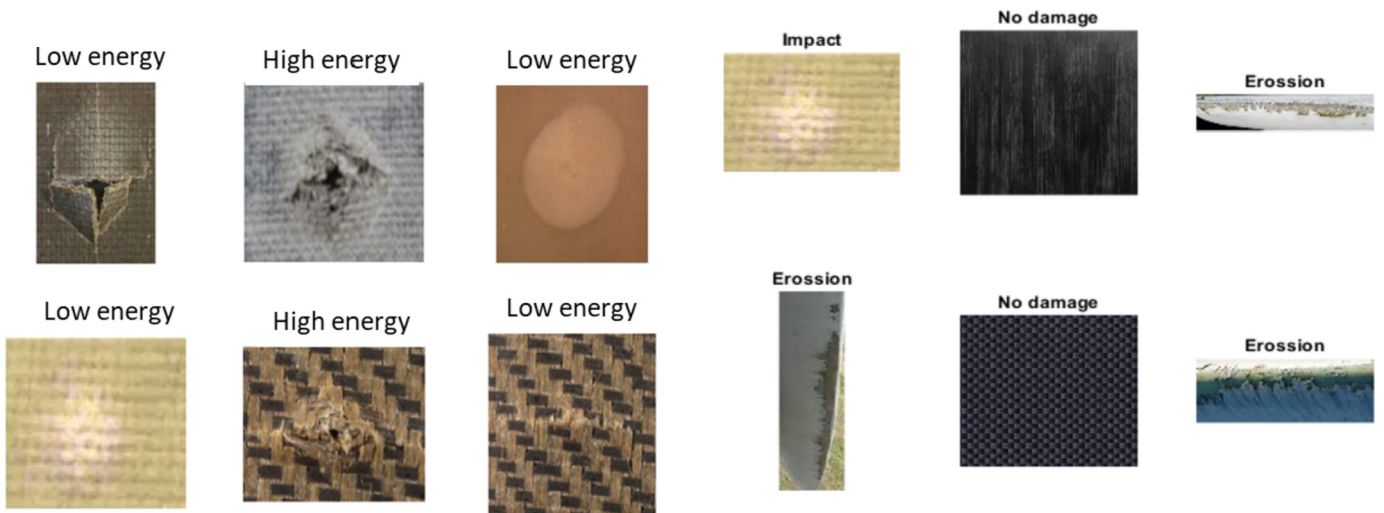


Fig. 30. Classification of damage severity for unseen images of the back face.

Fig. 32. Classification of validation images of macroscopic damage mechanisms.

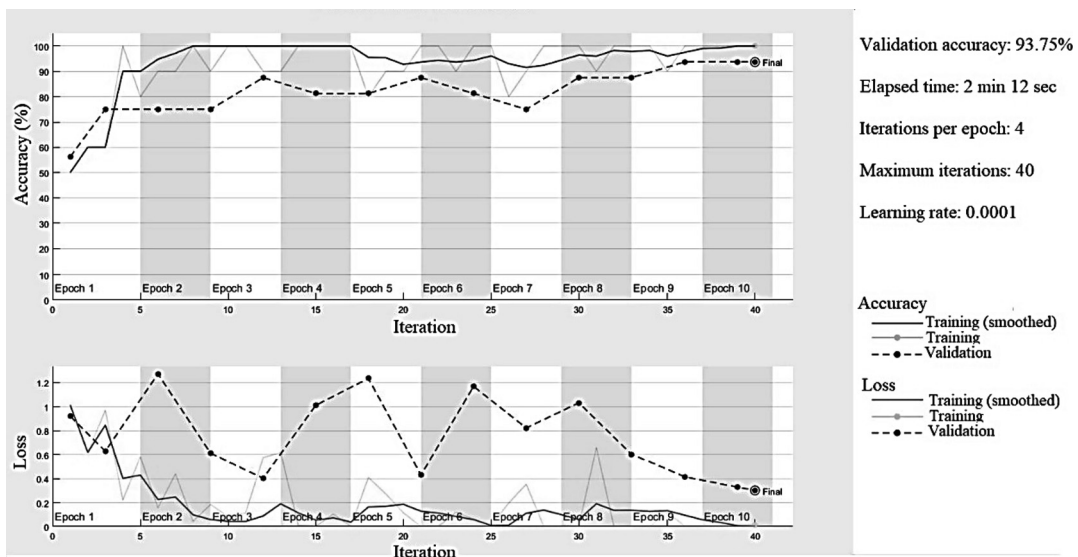


Fig. 31. Obtained validation accuracy for the classification of macroscopic damage mechanisms.

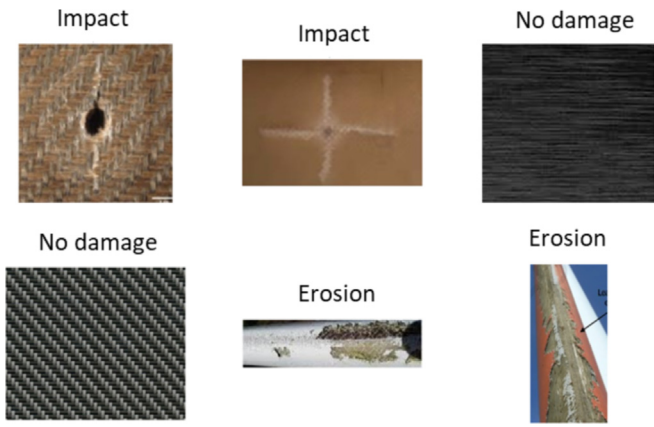


Fig. 33. Classification of unseen images of macroscopic damage mechanisms.

tures between the impacted face images and the back face images; where, there were not much obvious discrepancies between the images, so that the features extracted by the network were not distinct enough to yield accurate training and consequently reliable classification.

- The obtained results indicate the promising performance of deep learning to automate visual inspection, however it is highlighting the need for an improved dataset library, and customised classifiers for deep learning training.
- Future works could focus on developing comprehensive and high-quality datasets for different damage types in composite structures, and correlating the damage extent to the residual lifetime of the structure, making it possible to accurately train advanced deep learning algorithms for autonomous visual inspection purposes.

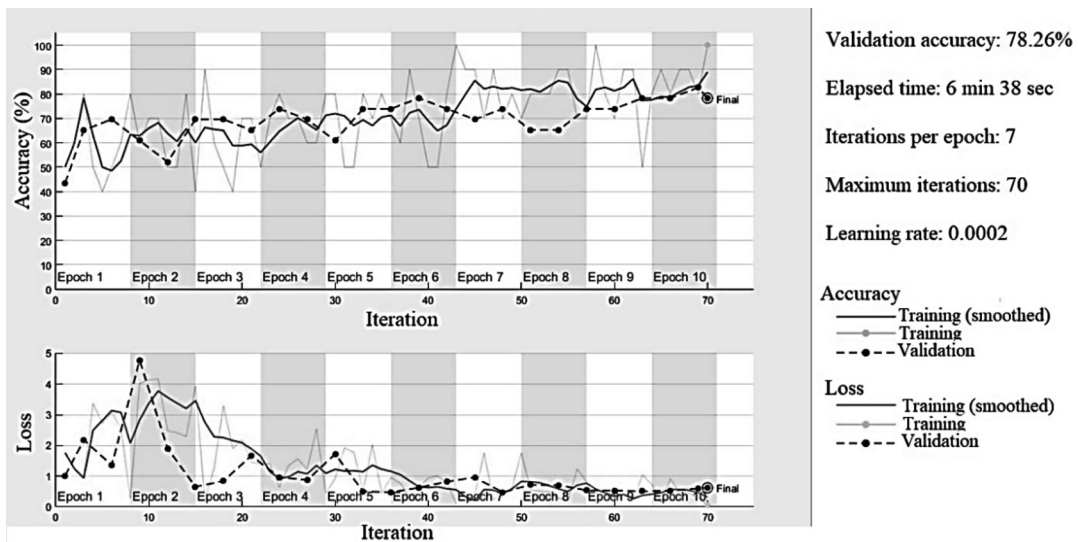


Fig. 34. Obtained validation accuracy for the classification of impacted and back faces (low energy impact).

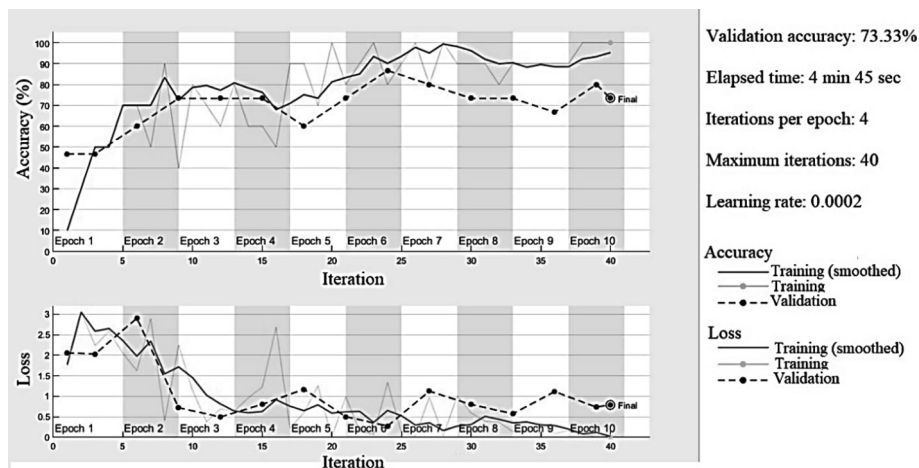


Fig. 35. Obtained validation accuracy for the classification of impacted and back faces (high energy impact).

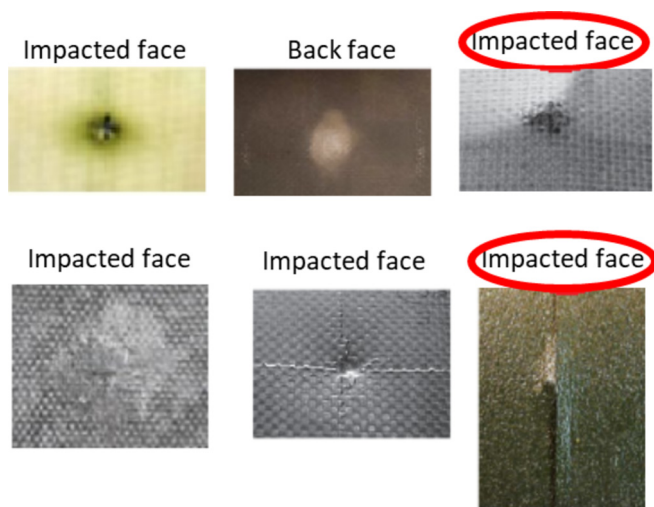


Fig. 36. Damage side classification of unseen images (low energy impact).

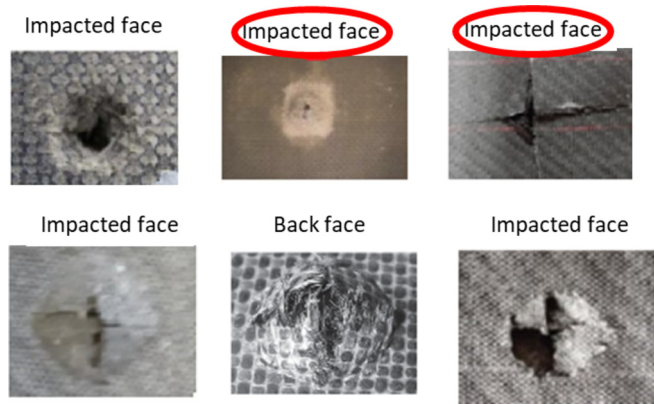


Fig. 37. Damage side classification of unseen images (high energy impact).

Declaration of Competing Interest

The authors declare that they have no known competing financial interests or personal relationships that could have appeared to influence the work reported in this paper.

Acknowledgements

This work was funded under the UK Engineering and Physical Sciences Research Council (EPSRC) Grant EP/V009451/1 on Next generation of high-performance impact resistant composites with visibility of damage. The data necessary to support the conclusions are included in the paper.

References:

- [1] Stewart R. Carbon fibre composites poised for dramatic growth. *Reinf Plast* 2009. [https://doi.org/10.1016/S0034-3617\(09\)70148-1](https://doi.org/10.1016/S0034-3617(09)70148-1).
- [2] Suwarta P, Fotouhi M, Czél G, Longana M, Wisnom MR. Fatigue behaviour of pseudo-ductile unidirectional thin-ply carbon/epoxy-glass/epoxy hybrid composites. *Compos Struct* 2019;224. <https://doi.org/10.1016/j.compstruct.2019.110996>.
- [3] Ogasawara T, Sugimoto S, Katoh H, Ishikawa T. Fatigue behavior and lifetime distribution of impact-damaged carbon fiber/toughened epoxy composites under compressive loading. *Adv Compos Mater* 2013. <https://doi.org/10.1080/09243046.2013.768324>.
- [4] Saeed MU, Chen Z, Chen Z, Li B. Compression behavior of laminated composites subjected to damage induced by low velocity impact and drilling. *Compos Part B Eng* 2014. <https://doi.org/10.1016/j.compositesb.2013.09.017>.
- [5] Cantwell WJ, Morton J. The impact resistance of composite materials - a review. *Composites* 1991. [https://doi.org/10.1016/0010-4361\(91\)90549-V](https://doi.org/10.1016/0010-4361(91)90549-V).
- [6] Sanchez-Saez S, Barbero E, Zaera R, Navarro C. Compression after impact of thin composite laminates. *Compos Sci Technol* 2005. <https://doi.org/10.1016/j.compscitech.2005.04.009>.
- [7] Talreja R, Singh CV. *Damage and failure of composite materials*; 2012.
- [8] Fotouhi S, Clamp J, Bolouri A, Pozegic TR, Fotouhi M. Investigating polyethersulfone interleaved Glass/Carbon hybrid composite under impact and its comparison with GLARE. *Compos Struct* 2019;226. <https://doi.org/10.1016/j.compstruct.2019.111268>.
- [9] Pashmforoush F, Fotouhi M, Sarhan AAD. Experimental–numerical study on minimizing impact induced damage in laminated composites under low-velocity impact. *J Reinf Plast Compos* 2018;37(3). <https://doi.org/10.1177/0731684417737166>.
- [10] Fotouhi M, Damghani M, Leong MC, Fotouhi S, Jalalvand M, Wisnom MR. A comparative study on glass and carbon fibre reinforced laminated composites in scaled quasi-static indentation tests. *Compos Struct* 2020. <https://doi.org/10.1016/j.compstruct.2020.112327>.
- [11] Heslehurst RB. *Defects and damage in composite materials and structures*; 2014.
- [12] Bossi RH, Giurgiutiu V. *Nondestructive testing of damage in aerospace composites. Polymer composites in the aerospace industry*, 2015.
- [13] Liu P, Groves RM, Benedictus R. 3D monitoring of delamination growth in a wind turbine blade composite using optical coherence tomography. *NDT E Int* 2014. <https://doi.org/10.1016/j.ndteint.2014.03.003>.
- [14] Peng W, Zhang Y, Qiu B, Xue H. A brief review of the application and problems in ultrasonic fatigue testing. *AASRI Procedia* 2012. <https://doi.org/10.1016/j.aasri.2012.09.024>.
- [15] Fotouhi M, Ahmadi Najafabadi M. Investigation of the mixed-mode delamination in polymer-matrix composites using acoustic emission technique. *J Reinf Plast Compos* 2014;33(19). <https://doi.org/10.1177/0731684414544391>.
- [16] Kroeger T. Thermographic inspection of composites. *Reinf Plast* 2014. [https://doi.org/10.1016/S0034-3617\(14\)70183-3](https://doi.org/10.1016/S0034-3617(14)70183-3).
- [17] Vavilov VP, Budadin ON, Kulkov AA. Infrared thermographic evaluation of large composite grid parts subjected to axial loading. *Polym Test* 2015. <https://doi.org/10.1016/j.polymertesting.2014.10.010>.
- [18] Tan KT, Watanabe N, Iwahori Y. X-ray radiography and micro-computed tomography examination of damage characteristics in stitched composites subjected to impact loading. *Compos Part B Eng* 2011. <https://doi.org/10.1016/j.compositesb.2011.01.011>.
- [19] Su Z, Zhou C, Hong M, Cheng L, Wang Q, Qing X. Acousto-ultrasonics-based fatigue damage characterization: linear versus nonlinear signal features. *Mech Syst Signal Process* 2014. <https://doi.org/10.1016/j.ymssp.2013.10.017>.
- [20] Bennett LGL, Lewis WJ, Hungler PC. The development of neutron radiography and tomography on a SLOWPOKE-2 reactor. 2013. doi: 10.1016/j.phpro.2013.03.003.
- [21] Yang SH, Kim KB, Oh HG, Kang JS. Non-contact detection of impact damage in CFRP composites using millimeter-wave reflection and considering carbon fiber direction. *NDT E Int* 2013. <https://doi.org/10.1016/j.ndteint.2013.03.006>.
- [22] S W. *Damage/Defect Types and inspection - some regulatory concerns*. MIL-17 Maint Work, no. July; 2006, p. 60–92.
- [23] Kujawińska A, Vogt K. Human factors in visual quality control. *Manag Prod Eng Rev* 2015. <https://doi.org/10.1515/mpcr-2015-0013>.
- [24] See JE. Visual inspection reliability for precision manufactured parts. *Hum Factors* 2015. <https://doi.org/10.1177/0018720815602389>.
- [25] Kostopoulos V et al. Autonomous inspection and repair of aircraft composite structures. *IFAC-PapersOnLine* 2018. <https://doi.org/10.1016/j.ifacol.2018.11.267>.
- [26] Canizo M, Onieva E, Conde A, Charramendieta S, Trujillo S. Real-time predictive maintenance for wind turbines using Big Data frameworks. 2017. doi: 10.1109/ICPHM.2017.7998308.
- [27] Zhou K, Fu C, Yang S. Big data driven smart energy management: From big data to big insights. *Renew Sustain Energy Rev* 2016. <https://doi.org/10.1016/j.rser.2015.11.050>.
- [28] Pernkopf F, O'Leary P. Image acquisition techniques for automatic visual inspection of metallic surfaces. *NDT E Int* 2003. [https://doi.org/10.1016/S0963-8695\(03\)00081-1](https://doi.org/10.1016/S0963-8695(03)00081-1).
- [29] Jiang F, Guan Z, Li Z, Wang X. A method of predicting visual detectability of low-velocity impact damage in composite structures based on logistic regression model. *Chinese J Aeronaut* 2021. <https://doi.org/10.1016/j.cja.2020.10.006>.
- [30] Jha SK, Bilalovic J, Jha A, Patel N, Zhang H. Renewable energy: present research and future scope of Artificial Intelligence. *Renew Sustain Energy Rev* 2017. <https://doi.org/10.1016/j.rser.2017.04.018>.
- [31] Azimi M, Eslamlou AD, Pekcan G. Data-driven structural health monitoring and damage detection through deep learning: state-of-the-art review. *Sensors (Switzerland)* 2020. <https://doi.org/10.3390/s20102778>.
- [32] Sony S, Laventure S, Sadhu A. A literature review of next-generation smart sensing technology in structural health monitoring. *Struct Control Health Monitor* 2019. <https://doi.org/10.1002/stc.2321>.
- [33] Krizhevsky A, Sutskever I, Hinton GE. ImageNet classification with deep convolutional neural networks. *Commun ACM* 2017. <https://doi.org/10.1145/3065386>.
- [34] Pour Rahimian F, Seyedzadeh S, Oliver S, Rodriguez S, Dawood N. On-demand monitoring of construction projects through a game-like hybrid application of BIM and machine learning. *Autom Constr* 2020. <https://doi.org/10.1016/j.autcon.2019.103012>.

- [35] Zeiler MD, Fergus R. Visualizing and understanding convolutional networks arXiv:1311.2901v3 [cs.CV] 28 Nov 2013. *Comput Vision–ECCV* 2014; 2014. doi: 10.1007/978-3-319-10590-1_53.
- [36] He K, Zhang X, Ren S, Sun J. Deep residual learning for image recognition. 2016. doi: 10.1109/CVPR.2016.90.
- [37] Saeed N, King N, Said Z, Omar MA. Automatic defects detection in CFRP thermograms, using convolutional neural networks and transfer learning. *Infrared Phys Technol* 2019. <https://doi.org/10.1016/j.infrared.2019.103048>.
- [38] Bang HT, Park S, Jeon H. Defect identification in composite materials via thermography and deep learning techniques. *Compos Struct* 2020. <https://doi.org/10.1016/j.compstruct.2020.112405>.
- [39] Gong Y, Shao H, Luo J, Li Z. A deep transfer learning model for inclusion defect detection of aeronautics composite materials. *Compos Struct* 2020. <https://doi.org/10.1016/j.compstruct.2020.112681>.
- [40] Meng M, Chua YJ, Wouterson E, Ong CPK. Ultrasonic signal classification and imaging system for composite materials via deep convolutional neural networks. *Neurocomputing* 2017. <https://doi.org/10.1016/j.neucom.2016.11.066>.
- [41] Khan A, Ko DK, Lim SC, Kim HS. Structural vibration-based classification and prediction of delamination in smart composite laminates using deep learning neural network. *Compos Part B Eng* 2019. <https://doi.org/10.1016/j.compositesb.2018.12.118>.
- [42] Su C et al. Improved damage localization and quantification of CFRP using lamb waves and convolution neural network. *IEEE Sens J* 2019. <https://doi.org/10.1109/JSEN.2019.2908838>.
- [43] Califano A, Chandarana N, Grassia L, D'Amore A, Soutis C. Damage detection in composites by artificial neural networks trained by using in situ distributed strains. *Appl Compos Mater* 2020. <https://doi.org/10.1007/s10443-020-09829-z>.
- [44] Tabian I, Fu H, Khodaei ZS. A convolutional neural network for impact detection and characterization of complex composite structures. *Sensors (Switzerland)* 2019. <https://doi.org/10.3390/s19224933>.
- [45] Jiao J, Zhao M, Lin J, Liang K. A comprehensive review on convolutional neural network in machine fault diagnosis. *Neurocomputing* 2020. <https://doi.org/10.1016/j.neucom.2020.07.088>.
- [46] Sony S, Dunphy K, Sadhu A, Capretz M. A systematic review of convolutional neural network-based structural condition assessment techniques. *Eng Struct* 2021. <https://doi.org/10.1016/j.engstruct.2020.111347>.
- [47] Unnikrishnan A, Sowmya V, Soman KP. Deep alexnet with reduced number of trainable parameters for satellite image classification. 2018. doi: 10.1016/j.procs.2018.10.342.
- [48] Mathworks help center, Transfer Learning Using AlexNet, R2021a. <https://uk.mathworks.com/help/deeplearning/ug/transfer-learning-using-alexnet.html>.
- [49] Ravandi M, Teo WS, Tran LQN, Yong MS, Tay TE. Low velocity impact performance of stitched flax/epoxy composite laminates. *Compos Part B Eng* 2017. <https://doi.org/10.1016/j.compositesb.2017.02.003>.
- [50] Sarasini F et al. Quasi-static and low-velocity impact behavior of intraply hybrid flax/basalt composites. *Fibers* 2019. <https://doi.org/10.3390/FIB2030026>.
- [51] Dong Fu H, ya Feng X, xu Liu J, ming Yang Z, He C, kui Li S. An investigation on anti-impact and penetration performance of basalt fiber composites with different weave and lay-up modes. *Def Technol* 2020. <https://doi.org/10.1016/j.dt.2019.09.005>.
- [52] Hosur MV, Adbullah M, Jeelani S. Studies on the low-velocity impact response of woven hybrid composites. *Compos Struct* 2005. <https://doi.org/10.1016/j.compstruct.2004.07.024>.
- [53] Selver E. Impact and damage tolerance of shear thickening fluids-impregnated carbon and glass fabric composites. *J Reinf Plast Compos* 2019. <https://doi.org/10.1177/0731684419842648>.
- [54] Shishevan FA, Akbulut H, Mohtadi-Bonab MA. Low velocity impact behavior of basalt fiber-reinforced polymer composites. *J Mater Eng Perform* 2017. <https://doi.org/10.1007/s11665-017-2728-1>.
- [55] Andrew JJ, Srinivasan SM, Arockiarajan A, Dhakal HN. Parameters influencing the impact response of fiber-reinforced polymer matrix composite materials: a critical review. *Compos Struct* 2019. <https://doi.org/10.1016/j.compstruct.2019.111007>.
- [56] Nogueira CL, De Paiva JMF, Rezende MC. Effect of the interfacial adhesion on the tensile and impact properties of carbon fiber reinforced polypropylene matrices. *Mater Res* 2005. <https://doi.org/10.1590/S1516-14392005000100015>.
- [57] Mitrevski T, Marshall IH, Thomson RS, Jones R. Low-velocity impacts on preloaded GFRP specimens with various impactor shapes. *Compos Struct* 2006. <https://doi.org/10.1016/j.compstruct.2006.06.033>.
- [58] Whittingham B, Marshall IH, Mitrevski T, Jones R. The response of composite structures with pre-stress subject to low velocity impact damage. *Compos Struct* 2004. <https://doi.org/10.1016/j.compstruct.2004.06.015>.
- [59] Petrucci R et al. Impact and post-impact damage characterisation of hybrid composite laminates based on basalt fibres in combination with flax, hemp and glass fibres manufactured by vacuum infusion. *Compos Part B Eng* 2015. <https://doi.org/10.1016/j.compositesb.2014.10.031>.
- [60] Ismail MF, Sultan MTH, Hamdan A, Shah AUM, Jawaid M. Low velocity impact behaviour and post-impact characteristics of kenaf/glass hybrid composites with various weight ratios. *J Mater Res Technol* 2019. <https://doi.org/10.1016/j.jmrt.2019.04.005>.
- [61] Sevkate E, Liaw B, Delale F, Raju BB. Drop-weight impact of plain-woven hybrid glass-graphite/toughened epoxy composites. *Compos Part A Appl Sci Manuf* 2009. <https://doi.org/10.1016/j.compositesa.2009.04.028>.
- [62] Kumari P, Wang J, Saahil. Residual tensile strength of the multi-impacted scarf-repaired glass fiber-reinforced polymer (GFRP) composites. *Materials (Basel)* 2018. <https://doi.org/10.3390/ma1122351>.
- [63] Tirillò J et al. High velocity impact behaviour of hybrid basalt-carbon/epoxy composites. *Compos Struct* 2017. <https://doi.org/10.1016/j.compstruct.2017.02.039>.
- [64] Shohag MAS, Hammel EC, Olawale DO, Okoli OI. Damage mitigation techniques in wind turbine blades: a review. *Wind Eng* 2017. <https://doi.org/10.1177/0309524X17706862>.
- [65] Chou JS, Chiu CK, Huang IK, Chi KN. Failure analysis of wind turbine blade under critical wind loads. *Eng Fail Anal* 2013. <https://doi.org/10.1016/j.engfailanal.2012.08.002>.
- [66] Bartolomé L, Teuwen J. Prospective challenges in the experimentation of the rain erosion on the leading edge of wind turbine blades. *Wind Energy* 2019. <https://doi.org/10.1002/we.2272>.
- [67] Ibrahim ME, Medraj M. Water droplet erosion of wind turbine blades: mechanics, testing, modeling and future perspectives. *Materials* 2020. <https://doi.org/10.3390/ma13010157>.
- [68] Cortés E, Sánchez F, O'Carroll A, Madramany B, Hardiman M, Young TM. On the material characterisation of wind turbine blade coatings: the effect of interphase coating-laminate adhesion on rain erosion performance. *Materials (Basel)* 2017. <https://doi.org/10.3390/ma10101146>.
- [69] Corsini A, Castorini A, Morei E, Rispoli F, Sciuili F, Venturini. Modeling of rain drop erosion in a multi-MW wind turbine. 2015. doi: 10.1115/GT2015-42174.
- [70] McElroy M, Jackson W, Olsson R, Hellström P, Tsampas S, Pankow M. Interaction of delaminations and matrix cracks in a CFRP plate, Part I: a test method for model validation. *Compos Part A Appl Sci Manuf* 2017. <https://doi.org/10.1016/j.compositesa.2017.09.011>.
- [71] Kreculj D, Rasuo B. Impact damage modeling in laminated composite aircraft structures. *Sustain Compos Aerospace Applications* 2018.
- [72] Tarpani JR, Milan MT, Spinelli D, Bose WW. Mechanical performance of carbon-epoxy laminates. Part II: quasi-static and fatigue tensile properties. *Mater Res* 2006. <https://doi.org/10.1590/S1516-14392006000200003>.
- [73] Brauer DS, Rüssel C, Vogt S, Weisser J, Schnabelrauch M. Degradable phosphate glass fiber reinforced polymer matrices: mechanical properties and cell response. *J Mater Sci - Mater Med* 2008. <https://doi.org/10.1007/s10856-007-3147-x>.
- [74] Jiang N, Sen Li D, qian Yao Q, wei Duan H, Ko F. Experimental study on compression properties and failure mechanism of 3D MWK carbon/epoxy composites at elevated temperatures. *Polym Compos* 2018. <https://doi.org/10.1002/pc.24372>.
- [75] Lafarie-Frenot MC, Hénaff-Gardin C, Gamby D. Matrix cracking induced by cyclic ply stresses in composite laminates. *Compos Sci Technol* 2001. [https://doi.org/10.1016/S0266-3538\(01\)00125-7](https://doi.org/10.1016/S0266-3538(01)00125-7).
- [76] Almansour FA, Dhakal HN, Zhang ZY. Effect of water absorption on Mode I interlaminar fracture toughness of flax/basalt reinforced vinyl ester hybrid composites. *Compos Struct* 2017. <https://doi.org/10.1016/j.compstruct.2017.02.081>.
- [77] Mathworks help center, ResNet-50 convolutional neural network. R2021a. <https://uk.mathworks.com/help/deeplearning/ref/resnet50.html>.
- [78] ImageNet. <http://www.image-net.org>.